Adhesive anchors in high performance concrete

Sara Cattaneo · Giovanni Muciaccia

Received: 26 February 2015 / Accepted: 13 July 2015

1 Introduction

The ever-increasing use of post-installed anchors is common both in retrofit and in new construction. Among the different types of fasteners, bonded anchors are very popular because of their flexibility.

For this reason, several research projects [7–10, 14, 16] have been conducted to study the experimental behavior of anchors and to propose simple design equations [5, 8, 13].

On the other hand, in recent years, high performance concrete (HPC) has been used in increasing volume [3, 4]. While the mechanical behavior of anchors in normal strength concrete has been studied for a long time, very limited attention has been devoted so far to HPC, some researches on bonded anchors considered the influence of the concrete strength on bond strength [9].

In theory, bonded anchors subject to tensile loads exhibit the same failure modes as mechanical anchors [9]. At small embedment depths a typical cone-shaped concrete breakout originating at the base of the anchor is observed. Increasing the embedment depth results in pull-out, which is characterized by a mixed-mode (bond/concrete breakout) failure, which is typical only of bonded anchors. This occurs either between mortar and concrete or between threaded rod and mortar. For larger embedment depths steel failure is observed.

S. Cattaneo (✉)
Department of Architecture, Built Environment and Construction Engineering, Politecnico di Milano, Piazza L. da Vinci 32, 20133 Milan, Italy
e-mail: sara.cattaneo@polimi.it

G. Muciaccia
Department of Civil and Environmental Engineering, Politecnico di Milano, Piazza L. da Vinci 32, 20133 Milan, Italy

Thus, the type of failure depends on the anchor embedment depth, the bond strength of the installed anchor, and on the strength of the steel and of the base material.

The evaluation of the ultimate load due to steel failure ($N_{R,s}$) is trivial as it depends only on the area of the threaded rod (A_s) and on the steel strength (f_{us}):

$$N_{R,s} = A_s \times f_{us} \tag{1}$$

On the other hand, the evaluation of the ultimate load for the other types of failure is quite challenging, as some aspects related to the bond between concrete and the bonding agent are still not clear.

The types of failure and the different models proposed in literature to predict the ultimate load of bonded anchors were thoroughly discussed by Cook et al. [9]. Authors classified the different approaches to predict the ultimate loads into six categories that could be roughly gathered: cone models (based on the concrete capacity design—CCD method), bond models and mixed cone–bond models. As a conclusion of their study they found that a uniform bond stress model provides the best fit of experimental data and agrees with non-linear analytical studies of adhesive anchor system (and it is user-friendly too). They clearly stated some limitations, and in particular the range of the concrete strength was between 13 and 68 MPa. Based on this investigation, other researches [10] moved on and nowadays this approach is widely accepted in codes and guidelines [1, 2, 12, 13, 15].

Indeed, according to current design method of bonded anchors, three different failure modes have to be accounted for (in this context splitting failure is neglected):

a. Steel failure (Eq. 1)
b. Combined pull-out and concrete cone failure
c. Concrete cone failure.

The resistance in case of combined pull-out and concrete cone failure, $N_{R,p}$ can be expressed as:

$$N_{R,p} = \pi \times d \times h_{ef} \times \tau_R \tag{2}$$

according to the bond model that assumes an uniform distribution of the bond stresses (τ_R) along the embedment depth (h_{ef}), d is the diameter of the rod.

Finally, the resistance of an anchor in case of concrete cone failure is given by:

$$N_{R,c} = k\sqrt{f_{ck,cube}} \times h_{ef}^{1.5} \tag{3}$$

according to the CCD approach [14], in ETAG [12] $k = 13.5$ for non-cracked concrete.

The design resistance of the bonded anchor is given by the lowest value of $N_{R,s}$, $N_{R,p}$ and $N_{R,c}$.

The bond strength τ_R depends on the bonding agents and could be defined only by tests.

Guidelines define two test configurations: confined and unconfined tests. The first is preferred in the American approach [2, 15] because they induce pull-out failure, but on the other hand the effect of confinement alters the ultimate load, and thus both ETAG [13] and ACI355.4 [12] take into account the boundary conditions through a reduction coefficient α_{setup}.

$$\tau_{Ru} = \alpha_{setup} \frac{N_u(C20/25)}{\pi \times d \times h_{ef}}, \tag{4}$$

where N_u is the failure load derived from testing in concrete C20/25.

In non-cracked concrete α_{setup} is equal to 1.0 if the tests are performed as unconfined tests or it is equal to 0.75 if the tests are performed as confined tests. In cracked concrete α_{setup} is equal to 0.70 if the tests are performed as confined tests.

Several studies have been performed to evaluate the influence of the concrete strength and of the anchor diameter or embedment depth/diameter ratio on the bond strength.

ACI 318-2011 [1] states that "bond strength is in general not highly sensitive to concrete compressive strength". However all guidelines suggest a strength normalization factor to take into account the compressive strength of the concrete which actually affects the ultimate load. The question is whether the bond strength is a characteristic value of the adhesive agent or changes with concrete strength. The objective of this work is to study the influence of powder addition (fly ash or microsilica), compressive strength and the addition of steel fibers on the behavior of bonded anchors subjected to tensile load and to shear load. A comparison between the experimental results and the standard rules is presented, as well as a discussion on the evaluation of the bond strength.

2 Experimental investigation

The experimental program considered two high-performance concretes designed for a compressive

strength, at 28 days, of about 75 and 90 MPa and a normal strength concrete (C20/25). The mix-design of HPC and the average compressive strength (f_{cm}), as well the cubic strength ($f_{c,cube}$), at the time of the test are reported in Table 1. The two strengths refer to the batch used for tensile tests and the batch used for shear and combined tension-shear tests. The compressive strength was evaluated on cores with diameter of 100 mm and a height of 200 mm (at least three for each composition) at the time of tests. The various concretes were made with an addition of different mineral admixtures: fly ash was added to the concrete with characteristic strength of 75 MPa, while microsilica was added to the mix with strength of 90 MPa. For each type of high performance concrete, two mixes were considered, plain and with steel hooked fibers with a length of 30 mm a diameter of 0.38 mm and an aspect ratio of 79. The normal concrete (according to EN206 [14]) was considered only for tensile tests and the average cubic compressive strength measured at the time of test was 24.4 MPa.

The specimens consisted of concrete blocks (1.25 × 1.25 × 0.30 m) in which several anchors were placed. Four hooks were positioned at the corners to allow the handling of the specimen. The anchors were spaced at a distance of 600 mm in order to avoid interaction between anchors and between anchors and handling hooks.

The fasteners consisted of a 12 mm threaded rod, with an ultimate characteristic strength f_{uk} of 500 MPa and a yielding characteristic strength f_{yk} of 400 MPa. An epoxy adhesive was used as bonding agent, injected with a two component "gun" type applicator. The components were mixed through a special mixing nozzle as they were dispensed.

All holes were drilled with a 14 mm bit using a rotary hammer drill and cleaned using a stiff brush and a vacuum cleaner according to manufacturer instructions. In tensile tests three different embedment depths were considered: 110 mm (according to manufacturer instructions), 75 and 50 mm. For the last two cases at least three tests were performed for each type of concrete, while for the nominal embedment length 110 mm one test was carried out for each concrete grade. Overall 30 unconfined tensile tests were performed. Shear tests for each concrete class were performed, a reference test at an edge distance of 55 mm (as the minimum edge distance indicated by the manufacturer) and three tests for a reduced edge distance of 40 mm, corresponding to almost three diameters. Additional tests were carried out in cases where different behaviour was observed. Overall 19 shear tests were performed. All the anchors subjected to shear tests were installed with an embedment depth of 110 mm.

The anchors were set and cured at ambient temperature (of about 20 °C).

During the tensile tests, load was applied by means of two hydraulic jacks with a reaction frame, with spherical hinges as support. Load was applied through a steel rod connected to the reaction frame at the top, and to a special fixture that connected to the anchor. The tensile tests were load controlled while the shear

Table 1 Mix-design and average compressive strength

	C75	C75F	C90	C90F
Cement CEM I 52,5 R (kg/m^3)	380	380	405	405
Fly ash (kg/m^3)	60	60	–	–
Microsilica in slurry 50 % (kg/m^3)	–	–	90	90
Sand + aggregates (kg/m^3)	1905	1905	1920	1920
Acrylic superplasticizer (l/m^3)	5.5	7	10	12
Water (l/m^3)	150	150	80	80
Steel fibers (kg/m^3)	–	50	–	70
f_{cm} (MPa) (Tension tests)	96.2	98.3	100.5	119.5
$f_{c,cube}$ (MPa) (Tension tests)	106.9	109.2	111.7	132.8
f_{cm} (MPa) (Shear/combined tests)	95.0	101.7	108.3	110.3
$f_{c,cube}$ (MPa) (Shear/combined tests)	105.6	120.3	113.0	122.6
Elastic modulus (MPa)	40,615	41,404	42,016	39,412
Standard deviation (MPa)	2.45	6.80	1.56	4.13

and combined load tests were conducted on a different testing frame specifically designed for anchor testing and were displacement controlled. During shear tests the load was applied parallel to the concrete surface, at a distance from the concrete surface of approximately 5 mm (Fig. 1). All data (load and displacements monitored by two LVDTs) were acquired with a HBM Spider8 data acquisition system.

3 Experimental results

3.1 Tensile tests

Depending on the anchor embedment length and on the type of concrete, three different failure modes were observed: steel failure (S) with the yielding and the rupture of the threaded rod, cone failure (C) and combined concrete cone and pull-out failure (C/P).

In Table 2 the results obtained for tensile (N) and shear (S) tests, each concrete grade and embedment depth are reported. Note that in the test code the first number refers to the type of concrete, while the second number indicates the embedment length. The failure mode, the average ultimate load and the standard deviation are reported.

At the nominal embedment depth (110 mm) steel failures, with average ultimate load similar to that given by manufacturer (57.6 kN) for a concrete grade C20/25, were found. Nevertheless, in high performance concrete, it seems that similar results can be obtained also with a reduced (75 mm) embedment depth, as shown in Fig. 2a, where the average ultimate loads as a function of the embedment depth for each concrete grade are shown.

Obviously, when steel failure occurred, the concrete grade did not affect the results. In all tests with fiber reinforced concrete (both C75F and C90F) and 75 mm embedment depth, steel failure was observed, while in plain concrete both steel and cone failures were detected, with similar values of the ultimate load (Fig. 2a). Tests on normal strength concrete show a significant reduction of the load (of about 25 %). Reducing the embedment depth to 50 mm in all cases cone failure was noted, and a correspondent reduction in the ultimate load was detected (Fig. 2a).

Fig. 1 Test setup in shear

3.2 Shear tests

Table 2 reports the results of shear tests for the different classes of considered concrete, indicating, for each test series, the edge distance, the failure type, the average value of ultimate loads and the standard deviation. In the code the first number refers to the type of concrete, while the second number indicates the edge distance (mm).

Usually failure occurred due to concrete edge failure (C) but, in some cases, fibers altered the behaviour and several cracks developed prior (C/S) or after steel failure (S/C).

By reducing the edge distance (from 55 to 40 mm), a reduction of the ultimate load by about 30 % was observed except for concrete C90F where it seems that this parameter slightly affects the results (only 9 % reduction of the ultimate load) (Fig. 2b).

4 Discussion

4.1 Influence of geometric parameters: embedment depth/edge distance

The embedment depth is a parameter considered only in tensile tests while the edge distance was considered for shear tests only.

In tensile tests with a reduction of the prescribed embedment depth of about 30 % (from 110 to 75 mm) steel or cone failure was observed with an overall behavior similar to failures observed in the control specimen (Table 2). However, a reduction of the embedment length of about 55 % (up to 50 mm) led to cone failure, with lower capacity and in some cases

Table 2 Maximum load and failure mode

Tensile load				
Code	h_{ef} (mm)	Failure mode	Ultimate average load N_u (kN)	Standard deviation (kN)
C25				
N-BD-25-75	75	C/P	46.30	0.60
C75 FA				
N-BD-75-50	50	C	35.23	1.73
N-BD-75-75	75	C/S	63.39	2.13
N-BD-75-110	110	S	61.88	–
C75F FA				
N-BD-75F-50	50	C	43.19	1.09
N-BD-75F-75	75	S	62.89	0.28
N-BD-75F-110	110	S	54.22	–
C90 MS				
N-BD-90-50	50	C	44.59	1.34
N-BD-90-75	75	C/S	60.44	5.29
N-BD-90-110	110	S	60.12	–
C90F MS				
N-BD-90F-50	50	C	50.67	2.49
N-BD-90F-75	75	S	60.77	6.17
N-BD-90F-110	110	S	64.68	–
Shear load				
Code	Edge distance in. (mm)	Failure mode	Ultimate average load N_u (kN)	Standard deviation (kN)
C75 FA				
S-BD-75-40	40	C	18.18	1.81
S-BD-75-55	55	C	25.46	
C75F FA				
S-BD-75F-40	40	C	21.83	3.01
S-BD-75F-55	55	S	32.00	
C90 MS				
S-BD-90-40	40	C	20.67	2.10
S-BD-90-55	55	C	29.24	
C90F MS				
S-BD-90F-40	40	C/S	30.85	2.19
S-BD-90F-55	55	C/CS	34.50	0.7

brittle failure (Fig. 3). In shear tests by increasing the edge distance higher ultimate loads were reported. However, under this load condition, the type of failure (concrete edge failure) did not change except for C90F, where steel failure was observed in one test only. Whatever the edge distance it seems that the brittle/ductile behavior of the anchors depends on the fibers (Fig. 4), indeed in concrete without fibers the behavior was brittle.

4.2 Influence of the concrete compressive strength

For the considered concrete classes, the tested anchors were expected to show steel failure at the average

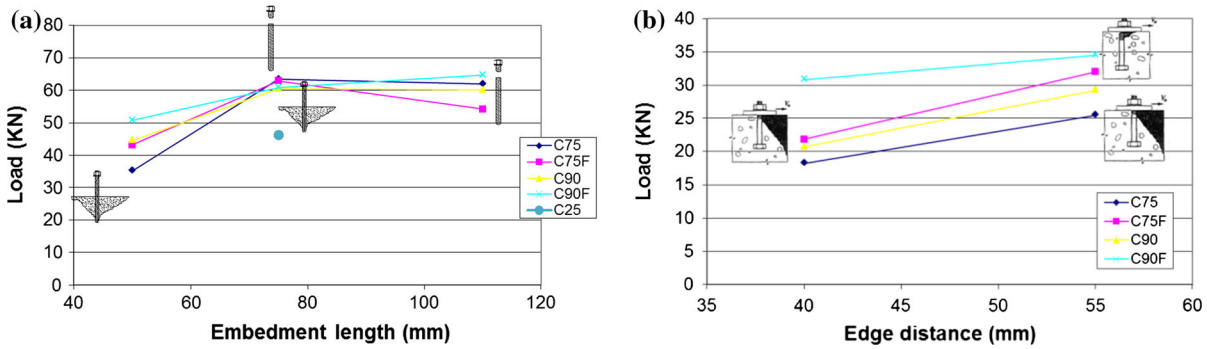

Fig. 2 Average ultimate load: tensile tests as a function of the embedment length (**a**) Shear tests as function of edge distance (**b**)

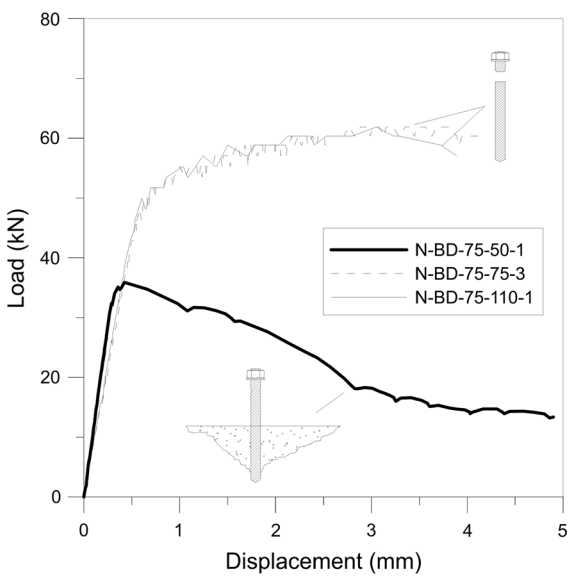

Fig. 3 Load–displacement curves for different embedment length: tensile tests (C75)

embedment depth prescribed by the manufacturer (110 mm). Thus, the effect of the compressive strength was evaluated by exploring reduced embedment depths/edge distances.

From a practical point of view, the higher compressive strength could potentially allow installation of the anchor even with reduced spacing/edge distance.

Figure 2a highlights that, unless steel failure is observed, the concrete grade can change the anchor capacity in tension in a significant manner. Compared to the ultimate load given by the manufacturer for steel failure (achieved for an embedment depth equal to 110 mm) it can be noted that by reducing the embedment depth (50 mm) the reduction of the ultimate load varied from about 12 % for the concrete C90F to about 39 % for the concrete C75.

The anchor subjected to shear load exhibits a similar behavior. Indeed, at the minimum edge distance (55 mm) all concretes showed a higher value

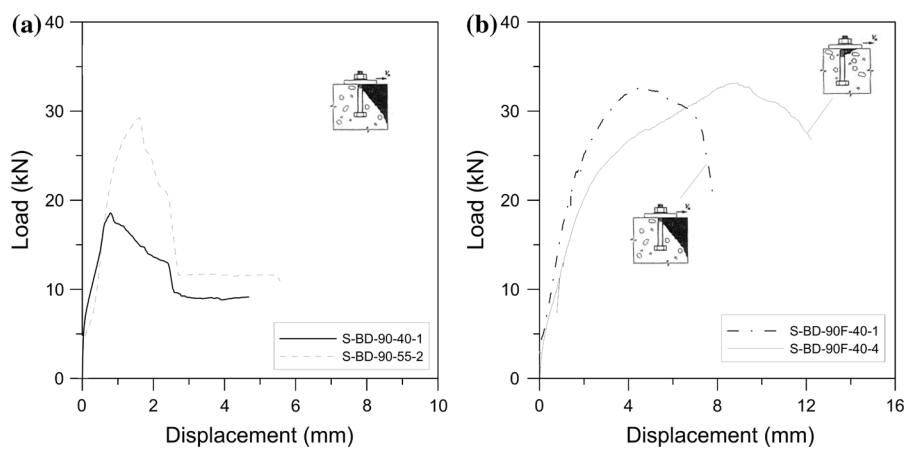

Fig. 4 Shear tests: load–displacement curves for different edge distance C90 (**a**) and C90F (**b**)

than the average value suggested by manufacturer at the critical edge distance (75 mm) where steel failure is expected.

By reducing the edge distance, a reduction of the ultimate load about 30 % was observed except for concrete C90F where it seems that this parameter slightly affects the results since steel failure can be reached even at reduced edge distance (40 mm).

4.3 Influence of fibers

As previously noted, the best performance was obtained with concrete C90F with fibers for both tensile and shear load. However, it is interesting to investigate, for the same concrete grade, the influence of the fibers on the ultimate load and on the overall behavior. Obviously a comparison of the effect of fibers can be done only when concrete failure occurs.

In tensile tests concrete failure was achieved for an embedment depth of 50 mm. By adding fibers to the mix, concrete C75 shows an increase of the ultimate load of about 18.5 %, while concrete C90 exhibits an increase of about 12 %.

The load displacement curves of specimens with fibers were characterized by a wide non-linear phase before the peak load (Fig. 5).

In addition, fibers change also the crack patterns and the cone dimensions. Figure 6 shows typical cones for plain (a) and fiber reinforced (b) concrete. The sketches of the crack pattern are drawn to scale, denoting that in fiber reinforced concrete, the cones were smaller.

Indeed, in plain concrete the cone developed starting from the tip of the threaded rod (concrete cone failure), while in fiber reinforced concrete the cone failure was combined with pull-out of about 10 mm of the threaded fastener (Fig. 6).

In shear tests fibers lead to an increase of the maximum load in all cases, but the rise is more noticeable for concrete C90 with the reduced edge distance of 40 mm (increase of about 33 %). A minimum increase of about 15 % was noticed.

As for tensile tests, the load displacement curves of specimens with fibers were characterized by a wide non-linear phase before the peak load (Fig. 7) and the post-peak behavior shows more softening. Fibers appear to reduce concrete cone dimensions and which may in turn prevent spalling of concrete as a result (Fig. 8).

5 Prediction models and experimental results

5.1 Tensile load

Guidelines [2, 11] assume a uniform bond stress distribution and give indications on how to evaluate the bond strength by means of tests, nevertheless some uncertainties are not completely solved.

The tests can be performed either in confined or unconfined conditions. In the first case pull-out failure is observed, but the result is affected by the confinement given by the test rig, thus guidelines attempt to mitigate the effect in confined tests by use of a reduction factor (a_{setup}).

In unconfined tests, a mixed cone-bond failure is usually detected. As noted in Cook [9], Meszaros [17] and McVay et al. [18], the uniform bond stress model has been shown to be appropriate for determining

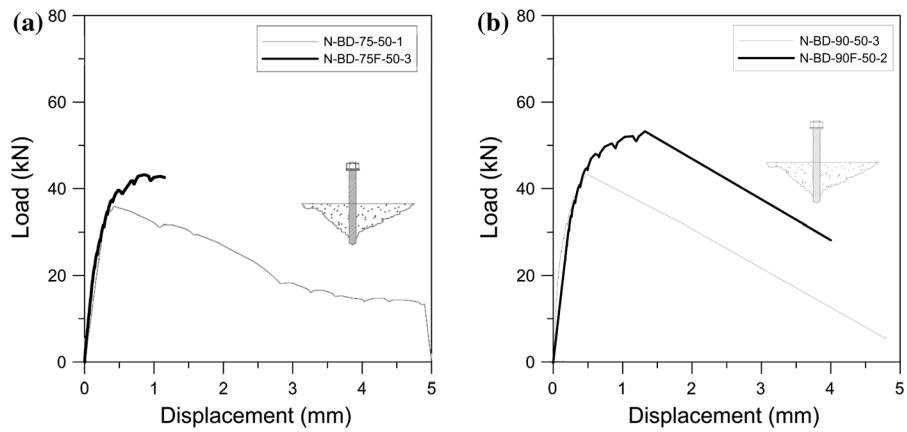

Fig. 5 Tensile tests—load–displacement curves: comparison plain–fiber reinforced concrete

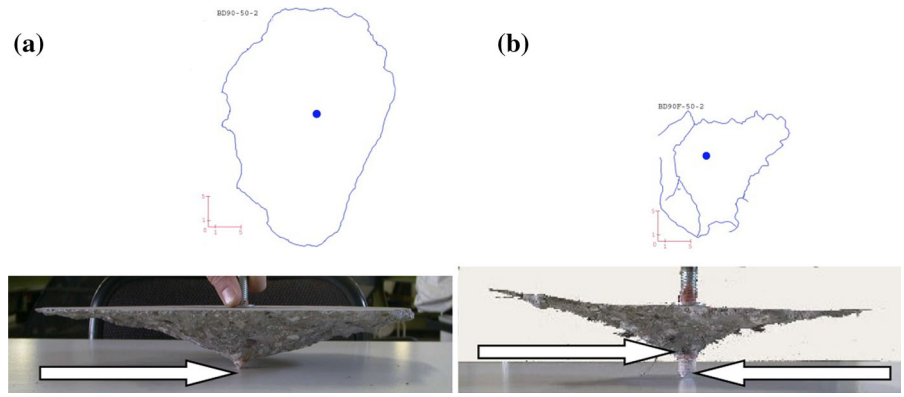

Fig. 6 Tensile tests: crack patterns and cones for plain (**a**) and fiber reinforced concrete (**b**)

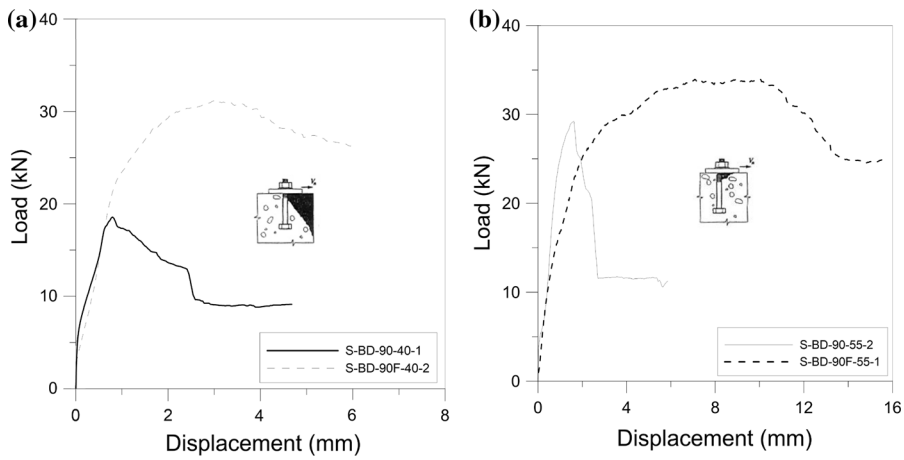

Fig. 7 Shear tests—load–displacement curves: comparison plain–fiber reinforced concrete

bond stress in unconfined applications within certain embedment length limitations (h_{ef} >70 mm according to [12]). In these studies, it has been shown that the shallow cone is a secondary failure. As an alternative, a mixed cone/bond model as introduced in Cook [8] and discussed in Cook et al. [9] but using the current concrete breakout equation (Eq. 3) for the contribution of the shallow cone might also be effective in determining bond strength.

According to the mixed-mode approach, the ultimate load can be evaluated as the sum of the two contributions: N_{cone}—the load given by the concrete cone (Eq. 3) with a cone height h_{cone} lower than h_{ef} and N_{bond}—the load given by the uniform bond stress (Eq. 2) over the length h_{ef}–h_{cone}:

$$N_u = N_{cone} + N_{bond} = 13.5 \times \sqrt{f_{ck,cube}} \times h_{cone}^{1.5} + \pi \times \tau \times d \times (h_{ef} - h_{cone})[N, mm] \quad (5)$$

The height of the concrete cone is obtained by minimizing [8] ($\partial N_u / \partial h_{cone} = 0$) the ultimate load:

$$h_{cone} = \left(\frac{\pi \times \tau \times d}{1.5 \times 13.5}\right)^2 \times \frac{1}{f_{ck,cube}} \quad (6)$$

The higher the bond strength the higher the value of h_{cone}, while the higher concrete strength $f_{ck,cube}$ the lower the value of h_{cone}.

However, researchers [7–10, 14, 16] and guidelines [2, 12] have shown that the uniform bond model is able to predict the ultimate load with good accuracy.

Table 3 reports all the tensile test results in which steel failure did not occur. The values predicted by considering the CCD approach (Eq. 3) and a modified CCD calibrated for HPC [6] are reported as well.

The values of $N_{R,c\ HPC}$ were evaluated according to Eq. (7)

$$N_{R,cHPC} = 4.62(f_{ck,cube})^{2/3} \times h_{ef}^{1.5}\ [N, mm] \quad (7)$$

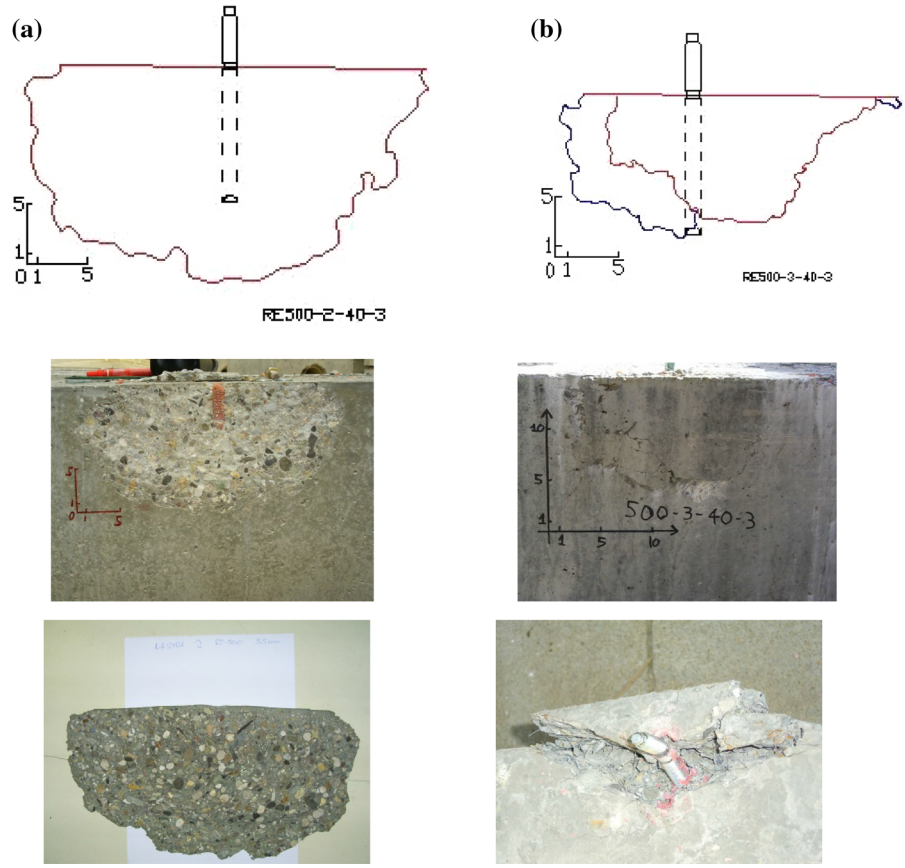

Fig. 8 Shear tests: crack patterns and cones for plain (**a**) and fiber reinforced concrete (**b**) (C90 and C90F)

that was derived from experimental tests on expansion anchors embedded in HPC [6].

The ratio between the experimental and predicted values is reported and shows that CCD approach adequately predicts the experimental results of normal strength concrete, while it tends to overestimate the load for HPC. On the other hand the modified CCD approach for HPC (Eq. 7) underestimates the ultimate load for normal strength concrete, while it is on the safe side (except for C75 and for C90 with larger embedment depth) for HPC.

Table 3 reports also the bond stress evaluated considering a uniform stress distribution (Eq. 2).

It can be noted that the obtained values are strongly dependent on the considered parameter (compressive strength, steel fiber, mineral addition, fly ash or microsilica), however while the ratio between the bond stress and the compressive strength is about 0.6 for normal concrete it drops between 0.17 and 0.21 for HPC.

Following the approaches previously suggested, the bond strength of the tested bonding agent was evaluated from the results of tests performed in C75 with an embedment depth of 50 mm (Table 3). By considering a uniform bond model (Eq. 2) the computed bond strength is $\tau = 18.7$ MPa.

Using the Eqs. (5) and (6) for the mixed cone/bond model, a cone depth of 13.6 mm and a bond strength of 20.5 MPa on the portion of the anchor experiencing bond failure can be determined. It should be noted that the mixed cone/bond model indicates a significant jump in bond stress at the depth of the shallow cone. In this example, the 13.6 mm shallow cone portion of the anchor transfers 7.0 kN by concrete breakout indicating that the bond stress in the top 13.6 mm is only 13.7 MPa while immediately below the shallow cone the bond stress jumps to 20.5 MPa.

The tests reported in Table 3 for concrete C20/25 ($f_{c,cube} = 24.4$ MPa) exhibited combined concrete cone/pull-out failure. From that results, by considering the Uniform Bond Model, the average bond resistance results equal to 16.4 MPa. By considering in a mixed formulation the bond strength to be 20.5 MPa on the

Table 3 Tensile tests (without steel failure): results and predictions

Code	h_{ef} (mm)	$f_{c,cube}$ (MPa)	Failure mode	Ultimate average load N_u (kN)	Concrete breakout, $N_{r,c}$ Eq. 3 (kN)	Concrete breakout, $N_{r,cHPC}$ Eq. 9 (kN)	$N_u/N_{r,c}$	$N_u/N_{r,cHPC}$	Uniform bond stress (MPa)
C25									
N-BD-25-75	75	24.4	C/P	46.3	43.3	25.2	1.07	1.83	16.4
C75-FA									
N-BD-75-50	50	106.9	C	35.2	49.3	36.8	0.71	0.96	18.7
C75F-FA									
N-BD-75F-50	50	109.2	C	43.2	49.9	37.3	0.87	1.16	22.9
C90-MS									
N-BD-90-50	50	111.7	C	44.6	50.4	37.9	0.88	1.18	23.7
N-BD-90-75[a]	75	111.7	C	60.4	92.7	69.6	0.65	0.87	21.4
C90F-MS									
BD-90F-50	50	132.8	C	50.7	55.0	42.5	0.92	1.19	26.9

[a] Average of two values, in the third test steel failure was observed

portion of the anchor below the calculated shallow cone depth of 60 mm, the predicted load is 42.6 kN versus the experimental value of 46.3 kN. Thus it seems that this approach is able to catch the behavior of ordinary concrete. It should be noted that as with the previous example the bond stress jumps from 13.7 to 20.5 MPa when assuming the mixed cone/bond model.

Finally, a comparison between the predictions of the previously presented models (Eqs. 2, 3, 5, 7) may be carried out. In Fig. 9 (top) the ratio between the experimental results and the predicted ones are reported as a function of the compressive strength for the different models. Figure 9 (bottom) shows the same data scaled over the range 100–140 MPa.

The behavior of normal strength concrete is well predicted by all models (except CCD for HPC—Eq. 7).

As previously discussed, it is shown how the CCD approach for HPC proposed in [6] for expansion anchors only is more suitable than the standard model also for bonded anchors.

The predictions of both the uniform bond model and the mixed cone/bond model are carried out adopting a value of bond strength computed from tests in low strength concrete and equal to 16.4 and

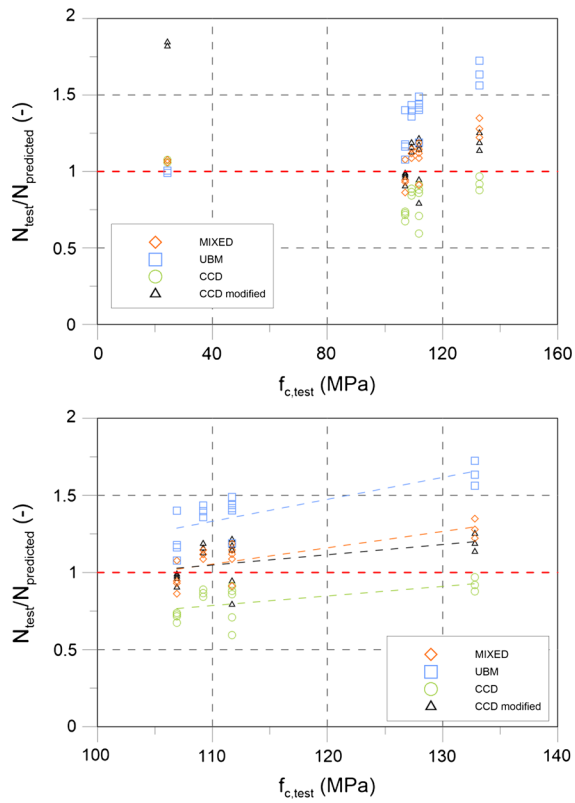

Fig. 9 Tensile tests: experimental data/model predictions

23.0 MPa for the two models, respectively. In the latter the value of bond strength equal to 23.0 MPa represents a limit value for a cone depth equal to the embedment depth and it assumes a bond strength of 15.3 MPa below the concrete cone.

In Fig. 9 the capacity predicted by the mixed cone–bond model are generally closer to the experimental values than any other model for all concrete classes except for C90F-MS, while the uniform bond model seems too conservative when the bond strength is not assumed to vary with the concrete compressive strength.

As concluding remark it may be noticed that the adoption of the Uniform Bond Model which assumes a unique value of bond acting below the shallow concrete cone which is independent on the concrete strength allows a good prediction of the anchor capacity whether the value of bond strength is calculated from tests in low strength concrete (23.0 MPa) or in high strength (20.5 MPa) concrete, as previously shown.

On the other hand, the value of bond strength predicted through a uniform bond model will depend on the concrete grade (in the investigated case equal to 16.4 MPa for C20 and to 18.7 MPa for C75-FA) and it will lead to conservative or unconservative prediction of the anchor capacity depending if the value estimated in low strength concrete is applied to high strength concrete or vice versa, respectively.

5.2 Shear load

Since the studies on shear behaviour of bonded anchors embedded in HPC are rather limited, it is interesting to compare the experimental results with the design equation that predict concrete edge failure presented in ETAG-Annex C [12]:

$$V_C = k_1 d^{\alpha} h_{ef}^{\beta} \sqrt{f_{ck,cube}}\, c_1^{1.5} [N, \text{mm}], \tag{8}$$

where $k_1 = 3$ for non-cracked concrete, c_1 is the edge distance, ℓ_f is the effective length of the anchor under shear load (here assumed).

$$\alpha = 0.1 \left(\frac{\ell_f}{c_1}\right)^{0.5} ; \quad \beta = 0.1 \left(\frac{d}{c_1}\right)^{0.2} \tag{9}$$

In Fig. 10 the ratio between the experimental results and the predicted ones are reported as a function of the compressive strength.

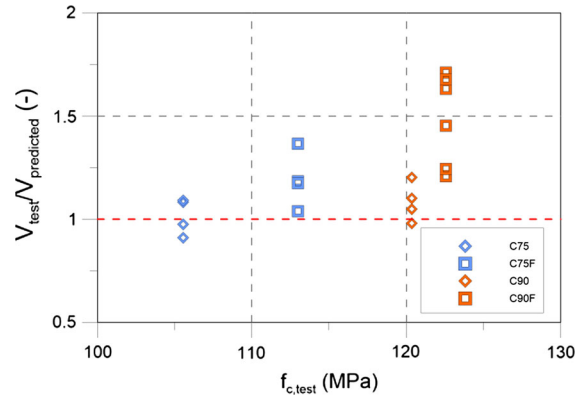

Fig. 10 Shear tests: experimental data/ETAG [12] prediction

It seems that design equation is able to properly predict the plain concrete behaviour, while the fiber reinforced concrete experimental results are underestimated. Nevertheless, the ratio raises the value of 1.7 for concrete C90F, and thus it can be stated that, based on this experimental campaign the existing design equation gives safe results.

6 Conclusions

An experimental investigation into the behavior of bonded anchors in HPC subject to tensile, shear and combined tensile-shear load was presented.

Test variables included concrete grade, addition of fly ash or microsilica, embedment length, incorporation of steel fibers and load direction.

From the study, the following conclusions may be drawn:

- In tensile tests the embedment depth corresponding to a transition from bond failure to cone failure decreases when increasing the concrete strength. For very low values of embedment depth (50 mm) fibers increase the ultimate load.
- Fibers lead to a combined cone-bond failure in tension and to the transition concrete to steel failure in shear tests by increasing the edge distance from 40 to 55 mm. In addition, for all load directions, smaller crack patterns were observed, suggesting useful applications when reduced edge distance or reduced anchor spacing are needed.

– Whatever the load directions the specimens with fibers exhibited a wide non-linear phase before the peak load. The specimens without fibers exhibited a more brittle behavior.
– ETAG [12] design equations for shear load seems to be suitable also for HPC.
– The proposed approach to evaluate the bond strength by the mixed cone/bond model seems to well predict the behavior of ordinary concrete while it seems to be too safe for HPC.

However, these results need further extended experimental investigations to be generalized.

References

1. ACI 318-2011 (2011) Building code and commentary. American Concrete Institute, Detroit
2. ACI 355.4-11 (2011) Qualification of post-installed adhesive anchors in concrete and commentary. American Concrete Institute, Farmington Hills, p 55
3. ACI Committee 363 (1992) 363R-92: state-of-the-art report on high-strength concrete, (Reapproved 1997). American Concrete Institute, Farmington Hills, p 55
4. Aïtcin PC (1998) High-performance concretes, construction and building materials. E & FN SPON, London, p 591
5. Biolzi L, Giuriani E (1990) Bearing capacity of a bar under transversal loads. Mater Struct 23(6):449–456
6. Cattaneo S (2007) Wedge-type expansion anchors in high-performance concrete. ACI Struct J 104(2):191–198
7. Cook RA, Konz RC (2001) Factors influencing bond strength of adhesive anchors. ACI Struct J 98(1):76–86
8. Cook RA (1993) Behavior of chemically bonded anchors. ASCE J Struct Eng 119(9):2744–2762
9. Cook RA, Kunz J, Fuchs W, Konz RC (1998) Behavior and design of single adhesive anchors under tensile load in uncracked concrete. ACI Struct J 95(1):9–26
10. Eligehausen R, Cook RA, Appl J (2006) Behavior and design of adhesive bonded anchors. ACI Struct J 103(6): 822–831
11. Ente Nazionale Italiano di unificazione UNI, EN206-1 (2006) Concrete—part 1: specification, performance, production and conformity. Milan, p 65
12. European Organisation for Technical Approval (EOTA), ETAG001 (1997) Guideline for European technical approval of metal anchors for use in concrete. Brussels, p 150
13. FIB Bulletin 58 (2011) Design of anchorages in concrete. FIB (Fédération Internationale du Béton/The International Federation for Structural Concrete), Lausanne, p 264
14. Fuchs W, Eligehausen R, Breen J (1995) Concrete capacity design (CCD) approach for fastening to concrete. ACI Struct J 92(1):73–94
15. ICC Evaluation Service, AC308 (2013) Acceptance criteria for post-installed adhesive anchors in concrete elements. ICC Evaluation Service, Whittier, p 61
16. Kunz J, Cook RA, Fuchs W, Spieth H (1998) Tragverhalten und bemessung von chemischen befestigungen. Beton und StahlebetonBau 93:H.1, pp. 15–19, H.2, pp. 44–49
17. Meszaros J (1999) Tragverhalten von Verbunddübeln im ungerissenen und gerissenen Beton (Load-bearing behavior of bonded anchors in uncracked and cracked concrete). Doctoral thesis, University of Stuttgart, (**in German**)
18. McVay M, Cook RA, Krishnamurthy K (1996) Pullout simulation of post-installed chemically bonded anchors. J Struct Eng ASCE 122(9):1016–1024